

## Electronic Supplementary Information

**Fabrication of Pt/Cu<sub>3</sub>(PO<sub>4</sub>)<sub>2</sub> ultrathin nanosheets  
heterostructure for photoelectrochemical microRNA sensing  
using novel G-wire-enhanced strategy**

Cui Ye,<sup>a</sup> Min Qiang Wang,<sup>b</sup> Ling Jie Li,<sup>c</sup> Hong Qun Luo,<sup>a\*</sup> and Nian Bing Li<sup>a\*</sup>

## 1. Chemicals and reagents

2-Amino-2-(hydroxymethyl)-1,3-propanediol (Tris), lactate oxidase (LOx) containing 41 units/mg solid was obtained from the Sigma Chemical Co. (St. Louis, MO). Lactic acid lithium salt, 6-mercaptohexanol (MCH), and  $\text{H}_2\text{PtCl}_6 \cdot 6\text{H}_2\text{O}$  were bought from Sigma-Aldrich (St. Louis, MO, U.S.A.). Silver nitrate ( $\text{AgNO}_3$ ), n-butyl alcohol ( $\text{C}_4\text{H}_{10}\text{O}$ ), copper nitrate ( $\text{Cu}(\text{NO}_3)_2 \cdot 6\text{H}_2\text{O}$ ), isooctane ( $\text{C}_8\text{H}_{18}$ ), and sodium dodecyl benzene sulfonate (SDBS) were purchased from Aladdin Industrial Co., Ltd. (Shanghai, China). Lambda exonuclease ( $\lambda$  exo) was purchased from New England BioLabs (U.S.A.). Diethylpyrocarbonate (DEPC)-treated deionized water was obtained from TaKaRa Biotechnology Co., Ltd (Dalian, China). Table S1† displays all oligonucleotides sequences, synthesized and purified by Sangon Inc. (Shanghai, China). All chemicals with analytical grade were used as received. Ultrapure water with a resistivity of 18.2 M $\Omega$  cm was used in whole work. The mixture of potassium ferricyanide and potassium ferrocyanide was dissolved in phosphate buffer (0.1 M KCl, 0.1 M  $\text{KH}_2\text{PO}_4$ , 0.1 M  $\text{Na}_2\text{HPO}_4$ , pH 7.4) to prepare ferricyanide solution ( $\text{Fe}(\text{CN})_6^{3-/4-}$ , 5 mM). The LOx stock solution (0.02 U  $\mu\text{L}^{-1}$ ) was prepared by dissolving 1.3 mg of lyophilized powder in phosphate buffer (2.5 mL, 0.1 M, pH 7.0).

## 2. Apparatus

The morphologies and structure were further characterized by a JEM-2100 field-emission scanning electron microscopy (FESEM) equipped with a field emission gun (FEG) at 200 kV on JEOL-7800F, and the energy-dispersive X-ray spectroscopy (EDS) was taken on INCA X-Max 250. (Japan Electron Optics Laboratory Co., Japan). The

Thermo ESCALAB 250Xi spectrometer was applied for X-ray photoelectron spectroscopy (XPS) analysis with a light source of Al K $\alpha$  X-ray (1486.6 eV) (Thermoelectricity Instruments, U.S.A.). The Brunauer–Emmett–Teller (BET) surface area was taken on Quadrasorb evo 2QDS-MP-30 with the adsorption gas of nitrogen (Quantachrome Instruments, U.S.A.). An XRD-7000 with Cu K $\alpha$  source radiation was used to investigate the X-ray diffraction pattern (XRD) at a scanning rate of 2° min<sup>-1</sup> from 10° to 80° (Shimadzu, Japan). A super digital thermostat bath of SD-101-005DB was used to maintain the experiment temperature (Sida Experimental Equipment Ltd., China). A xenon lamp parallel light source system of CHF-XM35-500W was applied for UV treatments, which coupled with a filter only allowing 365 nm UV transmissions (Beijing Trusttech Co. Ltd., China). Electrochemical and PEC measurements were respectively conducted on a CHI 660D electrochemical workstation (Shanghai Chenhua Instruments Co., China) and PEAC 200A (Tianjin AiDa Hengsheng Technology Co., Ltd., China). Three-electrode cell was used, including a platinum wire as a counter electrode, a modified glassy carbon electrode (GCE,  $\Phi$  = 3 mm) as a working electrode, and a saturated calomel electrode (SCE) as a reference electrode for electrochemical measurements or the Ag/AgCl for PEC measurements.

### **3. MiRNA analysis in cell lysates**

Human prostate carcinoma cells (22Rv1, high miRNA-141 expressions) and human cervical cancer cells (HeLa, low miRNA-141 expressions) were utilized for the practical sample analysis. Followed by cell counting, we use a column type commercial miRNA extraction kit to extract miRNA lysates from the cell samples.

Then those extracted miRNA lysates were diluted in 30  $\mu$ L of DEPC-treated ultrapure water.

#### **4. Optimal conditions for constructing PEC sensing platform**

To gain an optimal analytical performance of the PEC sensing platform, several possible factors influencing photocurrent generation are investigated. In this case, 0.5 nM miRNA is used as an example. As a well-designed protocol,  $\lambda$  exo is employed to assist helper probe reacting with target miRNA to release an intermediate C1, simultaneously realizing the target recycle for signal amplification. C1 with polyA tail can self-assemble onto the substrate, and then react with C2 to form a high-order G-wire superstructure with the help of  $K^+$  and  $Mg^{2+}$ , thus providing a plentiful sites to introduce  $P_{AgNCs@LOx-N_3}$  for exponential PEC signal amplification. Fig. S6a-c† depicts the influence of  $\lambda$  exo-assisted catalytic time, ligating C1 reaction time and G-wire formation time, respectively. Results indicate that the photocurrent responses increase with the augment of time. The optimal photocurrent response signals are gained after 60 min for  $\lambda$  exo-assisted catalysis, 3 h for ligating C1 reaction time, and 20 min for G-wire formation time. Furthermore, Apart from the above-mentioned time, the LOx labeled on signal probe can catalyze lactate to in site generate  $H_2O_2$ , which acted as an electron donor for further promoting PEC signal amplification. As displayed in Fig. S6d†, with increasing lactate concentration, the photocurrent increases rapidly and then levels off after 10  $\mu$ M. So, 10  $\mu$ M is employed as the optimal lactate concentration.

## 5. Additional data

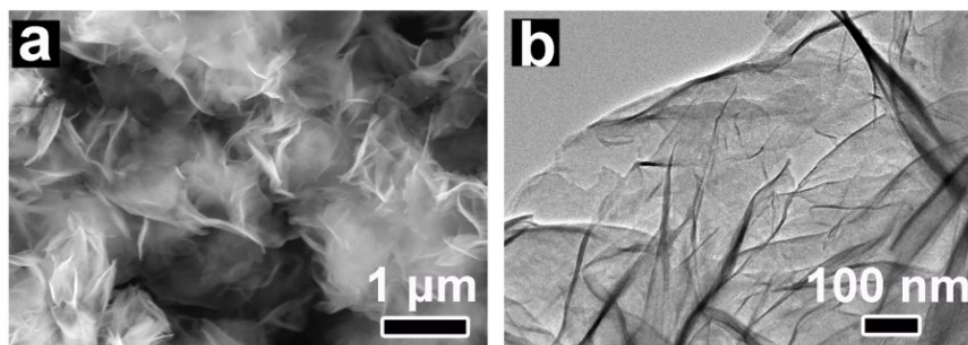


**Fig. S1.** a) SEM and b) TEM image of  $\text{Cu}_3(\text{PO}_4)_2\text{NSs}$ .

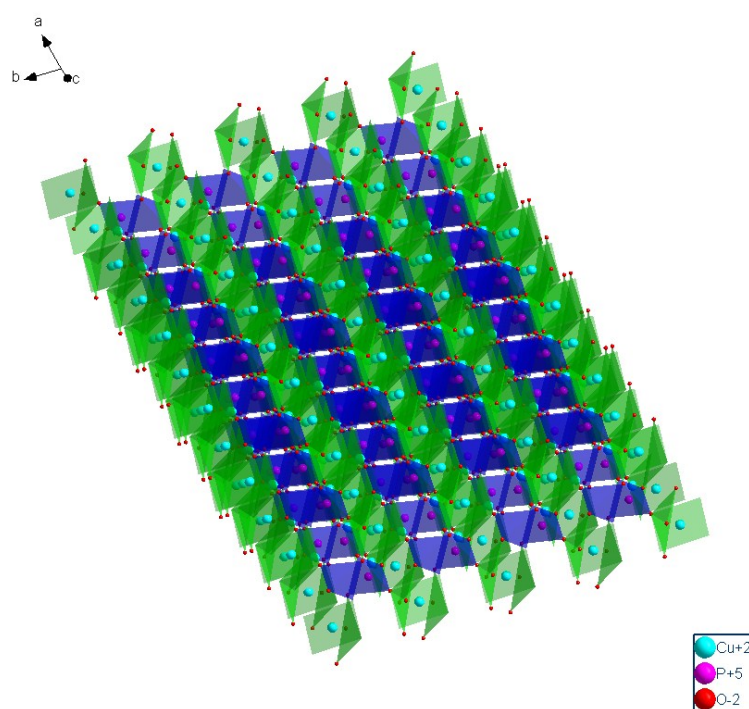


**Fig. S2.** Crystal structure of  $\text{Cu}_3(\text{PO}_4)_2$ .

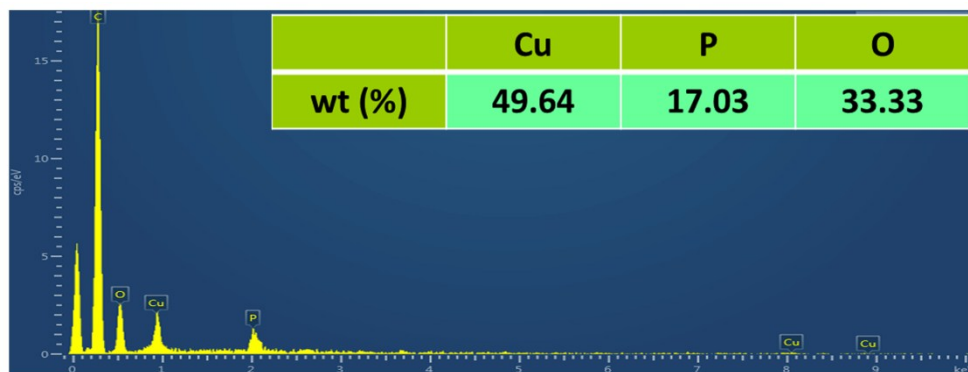


**Fig. S3.** EDS spectrum of  $\text{Cu}_3(\text{PO}_4)_2\text{NSs}$  (inset is weight percentage).

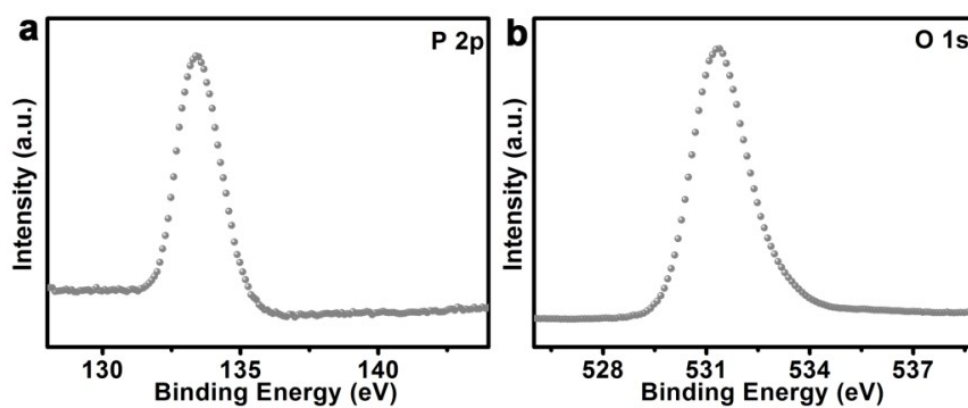


**Fig. S4.** XPS analysis of high-resolution spectra of a) P 2p and b) O 1s in PtNCs/ $\text{Cu}_3(\text{PO}_4)_2\text{NSs}$ .

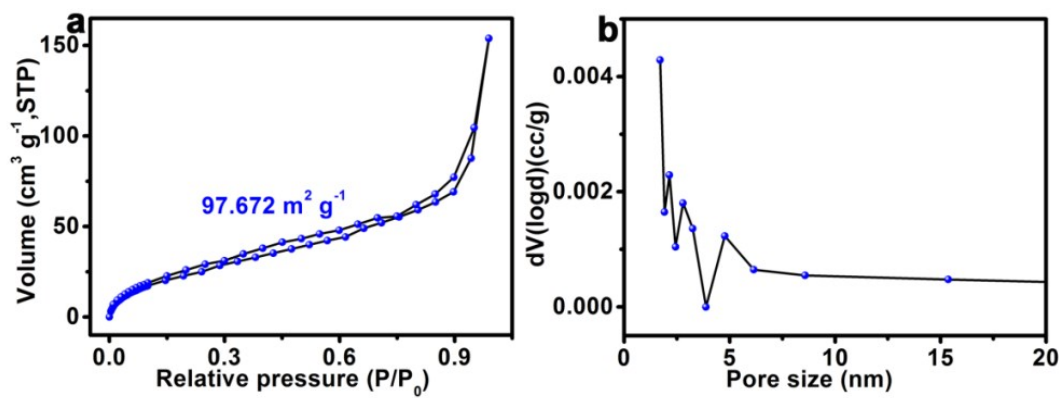


**Fig. S5.** a) Nitrogen adsorption-desorption and b) pore-size distribution isotherms of PtNCs/Cu<sub>3</sub>(PO<sub>4</sub>)<sub>2</sub>NSS.

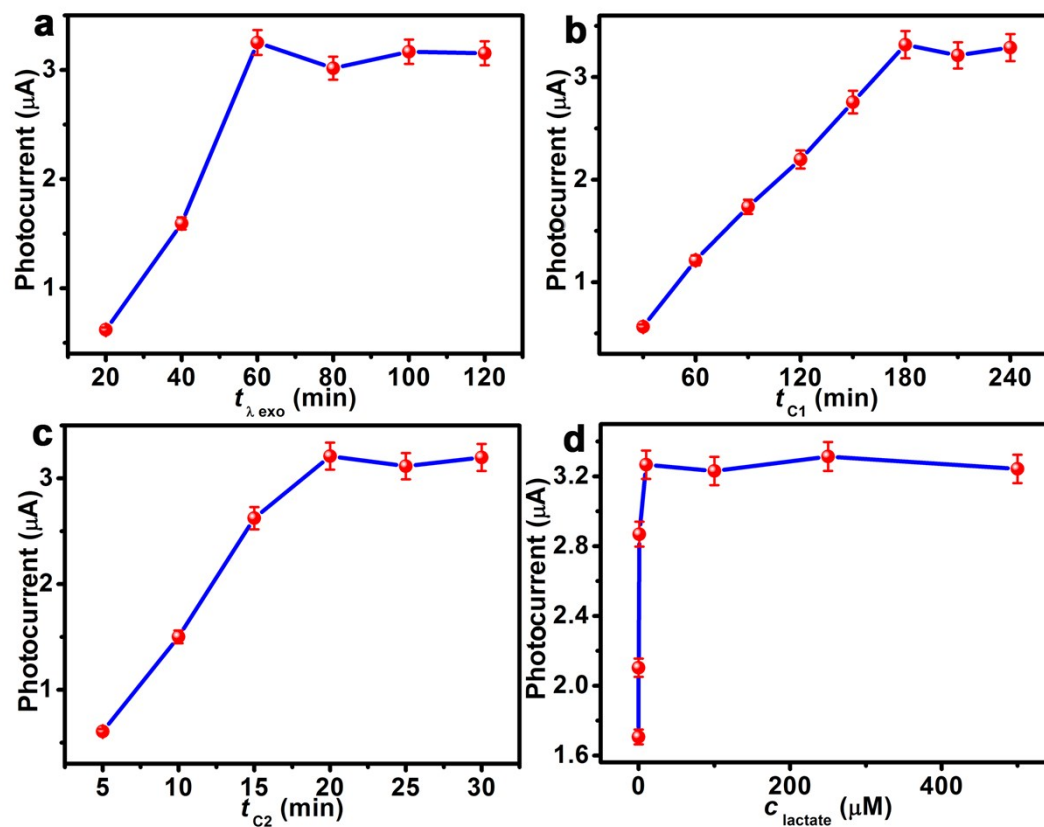


**Fig. S6.** Influences of a)  $\lambda$  exo-assisted catalytic time; b) ligating C1 reaction time; c) G-wire formation time; d) the lactate concentration.



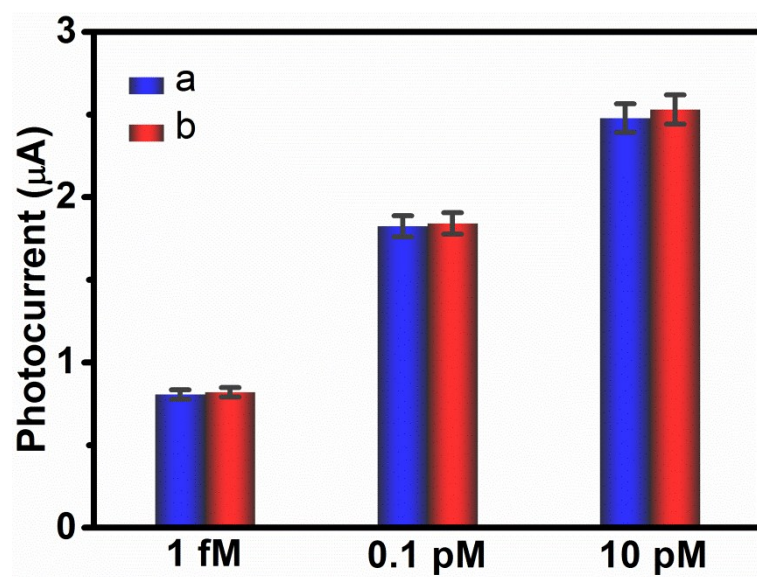


**Fig. S7.** Photocurrent responses of the prepared biosensor towards 0.001, 0.1, and 10 pM miRNA in (a) phosphate buffer and (b) lysates from  $10^2$  cells of HeLa containing lactate (4 mM, 10  $\mu$ L).

**Table S1.** Sequence information used in this work.

Name	Sequence (5'–3')
<b>MiRNA-141</b>	UAA CAC UGU CUG GUA AAG AUG G
<b>miR-200a</b>	UAACACUGUCUGGUAACGAUGU
<b>miR-200b</b>	UAAUACUGCCUGGUAUAUGAUGA
<b>miR-200c</b>	UAAUACUGCCGGGUAUAUGAUGGA
<b>miR-429</b>	UAAUACUGUCUGGUAUAACCGU
<b>c-myc</b>	DBCO-C <sub>6</sub> -AGGGTGGGGAGGGTGGGG-C <sub>6</sub> -DBCO
<b>Helper</b>	P- CCATCTTTACCAGACAGTGTATTTTTTTTTTCCCCA CAGGGTGGGGAGGGTGGGGAAAAAAAAAAAA
<b>Signal probe</b>	N <sub>3</sub> -AACTCGCCCTTAATCCCC

**Table S2.** XPS Spectra derived atomic percentages (%) and binding energy (eV) analysis for the PtNCs/Cu<sub>3</sub>(PO<sub>4</sub>)<sub>2</sub>NSs.

	<b>Cu</b>	<b>P</b>	<b>O</b>	<b>Pt</b>
<b>Atomic percentages (%)</b>	21.89	14.9	58.12	5.09
<b>Binding energy (eV)</b>	935.29	133.32	531.35	77.63

**Table S3.** Comparison with reported MiRNA detection methods.

Method	Detection limit (fM)	Dynamic range (fM - nM)	Ref.
<b>Fluorescence</b>	-	2000 - 10	[1]
<b>Fluorescence</b>	58	100 - 1	[2]
<b>Electrochemistry</b>	0.1	10 – 0.5	[3]
<b>Electrochemistry</b>	2	2 – 1	[4]
<b>ECL</b>	0.5	1 - 1	[5]
<b>ECL</b>	-	10 – 0.1	[6]
<b>PEC</b>	153	350 - 5	[7]
<b>PEC</b>	0.2	1 - 0.1	[8]
<b>PEC</b>	0.03	0.1 – 0.5	[9]
<b>PEC</b>	0.01	0.05 – 0.5	This work

## References

- [1] Z. Zhang, Y. Wang, N. Zhang, S. Zhang, *Chem. Sci.* 2016, **7**, 4184.
- [2] L. Wang, R. Deng, J. Li, *Chem. Sci.* 2015, **6**, 6777.
- [3] T. Wang, E. Viennois, D. Merlin, G. Wang, *Anal. Chem.* 2015, **87**, 8173.
- [4] C. S. Fang, K. S. Kim, B. Yu, S. Jon, M. S. Kim, H. Yang, *Anal. Chem.* 2017, DOI: 10.1021/acs.analchem.6b04609.
- [5] Q. M. Feng, Y. Z. Shen, M. X. Li, Z. L. Zhang, W. Zhao, J. J. Xu, H. Y. Chen, *Anal. Chem.* 2016, **88**, 937.
- [6] Y. Y. Zhang, Q. M. Feng, J. J. Xu, H. Y. Chen, *ACS Appl. Mater. Interfaces*, 2015, **7**, 26307.
- [7] W. Tu, H. Cao, L. Zhang, J. Bao, X. Liu, Z. Dai, *Anal. Chem.* 2016, **88**, 10459.
- [8] Z. Y. Ma, F. Xu, Y. Qin, W. W. Zhao, J. J. Xu, H. Y. Chen, *Anal. Chem.* 2016, **88**, 4183.
- [9] C. Ye, M. Q. Wang, Z. F. Gao, Y. Zhang, J. L. Lei, H. Q. Luo, N. B. Li, *Anal. Chem.* 2016, **88**, 11444.